Available online at www.sciencedirect.com
SCIENCE DIRECT®
Journal of Magnetic Resonance 172 (2005) 56–62
JMR Journal of Magnetic Resonance
www.elsevier.com/locate/jmr

Resolution enhancement in MAS solid-state NMR by application of ^{13}C homonuclear scalar decoupling during acquisition

Veniamin Chevelkov[a,b], Zhongjing Chen[a,b], Wolfgang Bermel[c], Bernd Reif[a,d,*]

[a] *Forschungsinstitut für Molekulare Pharmakologie, Robert-Roessle-Str. 10, 13125 Berlin, Germany*
[b] *Institut für Organische Chemie und Biochemie II, TU München, Lichtenbergstr. 4, D-85747 Garching, Germany*
[c] *Bruker BioSpin GmbH, Silberstreifen 4, D-76287 Rheinstetten, Germany*
[d] *Charité Universitätsmedizin, D-10115 Berlin, Germany*

Received 30 June 2004; revised 20 September 2004

Abstract

Spectral resolution imposes a major problem on the evaluation of MAS solid-state NMR experiments as larger biomolecular systems are concerned. We show in this communication that decoupling of the ^{13}C–^{13}C homonuclear scalar couplings during stroboscopic detection can be successfully applied to increase the spectral resolution up to a factor of 2–2.5 and sensitivity up to a factor of 1.2. We expect that this approach will be useful for the study of large biomolecular systems like membrane proteins and amyloidogenic peptides and proteins where spectral overlap is critical. The experiments are demonstrated on a uniformly ^{13}C,^{15}N-labelled sample of Nac-Val-Leu-OH and applied to a uniformly ^{13}C,^{15}N-enriched sample of a hexameric amyloidogenic peptide.
© 2004 Elsevier Inc. All rights reserved.

Keywords: High resolution MAS solid-state NMR; Homonuclear scalar decoupling; Spectral resolution and sensitivity; Adiabatic pulses

1. Introduction

Structure investigations of non-crystalline solids by high resolution solid-state NMR made rapid progress during the last few years. These investigations recently resulted in complete structure elucidation of several peptides and small proteins [1,2]. Successful spectral assignment and determination of structural constrains in isotopically enriched materials (mostly ^{13}C, ^{15}N) is still limited by resolution and sensitivity. Limited resolution hampers application of current solid-state NMR techniques to larger important biological systems beyond 8 kDa, like many membrane proteins. In the past, many methods have been developed to suppress strong anisotropic interactions and improve line width in solid-state NMR, like sample preparation [3], fast and ultra-fast MAS [4,5], development of hetero- and homonuclear dipole–dipole decoupling sequences [6–8], and sensitivity enhancement schemes making use of the high gyromagnetic ratio of the detected spin [9–12]. These developments resulted in significant line narrowing making scalar homonuclear couplings the major determinants of the ^{13}C line width in uniformly enriched samples.

The achievable line width of ^{13}C without J decoupling is on the order of 100–150 Hz [13], while typical one bond J-coupling constants in amino acids are 55 Hz for C_α–C' and 35 Hz for C_α–C_β [14,15]. In addition, $^{3}J_{cc}$ couplings between backbone and side chain carbons yield an additional contribution to the observed line width. Removal of these couplings is getting more and more important in solid-state NMR as higher quality spectra are obtained.

^{13}C,^{13}C homonuclear decoupling can be achieved either by application of selective radiofrequency pulse schemes or biosynthetically by using a labelling strategy

* Corresponding author. Fax: +493094793199.
E-mail address: reif@fmp-berlin.de (B. Reif).

1090-7807/$ - see front matter © 2004 Elsevier Inc. All rights reserved.
doi:10.1016/j.jmr.2004.09.017

in which each ^{13}C is only directly bonded to ^{12}C nuclei. A number of approaches to achieve J decoupling which were originally developed in solution-state NMR have successfully been implemented in solid-state NMR. Selective ^{13}C labelling schemes [1,16,17] remove J couplings and also reduce dipolar truncation effects, facilitating long range distance determination. On the other hand, uniform ^{13}C labelling of the backbone is required for sequential assignments. Application of selective pulses for refocusing homonuclear J coupling in the indirect dimension was used in solution NMR [18]. This idea was implemented in solid-state NMR by Straus et al. [19] and later reconsidered by Igumenova et al. [20] to decouple ^{13}C. These approaches were limited so far to the indirect dimension, while the direct dimension would be more efficient in terms of experimental time expenses. Combination of decoupling in both the direct and indirect dimensions should yield, however, the best resolution.

Recently, Emsley and co-workers [21,22] applied spin-state selective excitation schemes in solid-state NMR, which were originally developed by Sørensen and co-workers [23] for solution-state NMR. Single and double IPAP selection filters were used for 1D experiments to separate a single multiplet component by recording and superposition of in- and anti-phase doublet and quartet spectra [22]. In the 2D ^{13}C,^{13}C correlation experiment, a quite elegant scheme was employed [21] where spin-state selection in the indirect dimension was achieved using an IPAP sequence within a constant time ^{13}C evolution period, while PDSD is used as a zero-quantum mixing sequence to obtain spin-state selective C'–C_α polarization transfer, yielding line narrowing in the direct dimension after combination of interleaved recorded data sets with one another. The major prerequisite are relatively long filtering time periods on the order of $1/2J$ often resulting in significant polarization losses at moderate MAS frequencies. The experiment demonstrates a remarkable improvement in resolution in the direct dimension by as much as 44%, while the line width in the indirect dimension was enhanced by 17%. The last value was achieved due to a relatively short t_1^{max}, which was a compromise between loss of polarization (ca. 35%) and line width. To extract the single spin component, an empirical scaling factor has to be employed to combine the different data sets [21]. This empirical scaling factor is linked to the PDSD mixing time, which does not transfer the same way the in- and anti-phase signals. This practical complication makes application of spin-state selective experiments for correlation spectroscopy less convenient.

Carbon–carbon scalar couplings can also be removed by selective irradiation of one or several spectral regions of interacting nuclei. In this case, the respective multiplet collapses into a single resonance line. Such decoupling techniques are used for decoupling in the indirect dimension in solution-state NMR, employing wide band selective adiabatic pulses [24,25]. Band selective homonuclear carbon–carbon decoupling can be applied during ^{13}C acquisition. This approach has recently been successfully implemented for ^{13}C detection of paramagnetic proteins [26] in solution-state NMR.

In the present work, we implement a mono and double band selective homonuclear J decoupling sequence based on selective irradiation in the direct dimension to increase the effective resolution for solid-state NMR applications. We show that the application of a weak RF field does not interfere with sample rotation if care is taken to avoid HORROR ($\omega_{RF} = \omega_{rot}/2$) [27] or R3 ($\omega_{RF} = n\omega_{rot}$) [28] conditions. The method was tested first using a uniformly ^{13}C, ^{15}N enriched peptide sample, Nac-Val-Leu-OH, and was then applied to an amyloidogenic hexameric peptide (STVIIE), where severe overlap in the C_α and C' spectral region prevented the assignment of these resonances.

2. Experimental

All experiments were carried out on a 600 MHz Bruker-Avance spectrometer, equipped with a 4 mm triple resonance probe. The employed 1D and 2D pulse schemes are illustrated in Fig. 1. We assume that all anisotropic interactions as well as ^{13}C–^{1}H scalar couplings were reduced to an insignificant level by MAS (ca. 11–12.5 kHz) and application of TPPM proton decoupling using a RF field strength of ca. 90 kHz. All experiments start with a 90° ^{1}H excitation pulse followed by a ramped CP magnetization transfer from

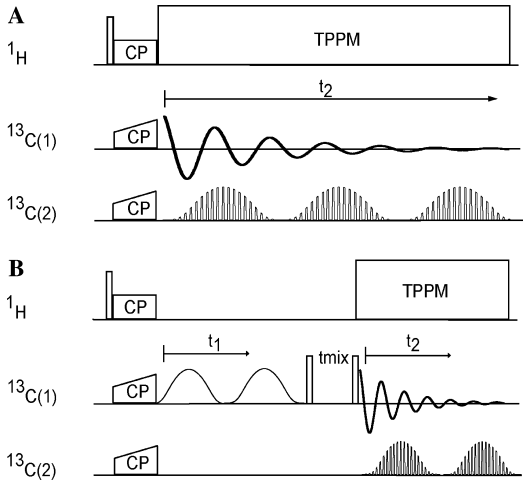

Fig. 1. (A) Pulse sequence employed for ^{13}C–^{13}C homonuclear scalar decoupling during detection. Selective pulses with windows for data sampling are represented as shapes with gaps and 90° pulses are indicated by open bars. (B) 2D ^{13}C–^{13}C PDSD pulse scheme with ^{13}C–^{13}C homonuclear decoupling during detection. Selective irradiation in the indirect dimension is represented as a shape.

protons to carbon. In the 2D experiment, C′ is selectively irradiated during the evolution in the indirect dimension to suppress the scalar coupling to C_α. Proton driven spin diffusion is used to yield magnetization transfer between different carbon sites. In all experiments, band-selective homonuclear $^{13}C,^{13}C$ scalar decoupling was achieved during stroboscopic detection by application of band-selective adiabatic RF pulses. To avoid misunderstandings hereafter, we use the term "stroboscopic/windowed detection" to refer to a acquisition mode in which the amplifier is open during HDDUTY and blanked during the remaining dwell time in order to acquire a sampling point. This results in an increased noise level. In contrast, the expression "standard detection" is used to denote an acquisition mode in which the amplifier is blanked at all times during detection.

The window duration for irradiation (HDDUTY) was set to 37% of the dwell time, as a compromise between decrease of the signal-to-noise ratio due to probe ring down and efficiency of the decoupling performance. In the experiments, a dwell time of 14.7 μs was employed. A supercycled adiabatic SEDUCE-1 (digitized into 1000 points) pulse [29,30] was used to irradiate the selected frequency band(s), generating a "DANTE-like" [31] train facilitating the selectivity of the shaped pulse. In the stroboscopic regime at low power, the signal-to-noise ratio depends on HDDUTY according to [26]

$$\frac{S}{N} = \frac{S}{N}\bigg|_0 \sqrt{1 - \frac{\mathrm{HDDUTY}}{100}} \tag{1}$$

yielding 0.79 for a HDDUTY value of 37%. Experimentally, we observe however a smaller value: the signal-to-noise ratio measured at HDDUTY of 37% and zero power is reduced to 0.65 compared to conventional detection. However, collapse of multiplets into singlets still yields a sensitivity improvement.

For a quantitative characterization of band-selective homodecoupling, the uniformly ^{13}C, ^{15}N-labelled dipeptide Nac-Val-Leu-OH was used as a test sample. The MAS frequency was set to 12.5 kHz. All experiments were carried out at 280 K. Fig. 2 shows several experimental ^{13}C-1D spectra, in which no decoupling was applied (A,D,F), C_α was decoupled from C′ (B), C_α was simultaneously decoupled from C′ and C_β (C), and C′ was decoupled from C_α (E). MLEV16 [32] and P9 [33,34] supercycling of the selective pulses was used in

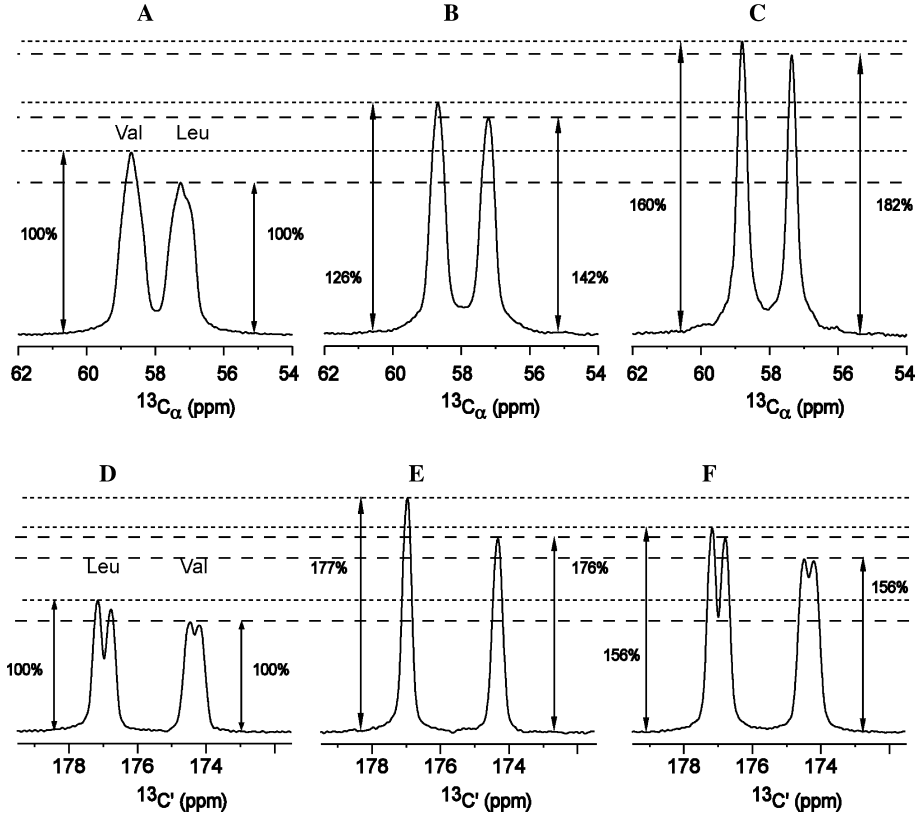

Fig. 2. ^{13}C-1D spectra of u-[^{13}C–^{15}N]Nac-Val-Leu-OH, displaying the $^{13}C'$ and $^{13}C_\alpha$ spectral regions. The MAS frequency was adjusted to 12.5 kHz. The acquisition time was set to 50 ms. The signal was processed without any apodization. The same experimental conditions were used in all experiments to allow for direct comparison of resolution and the signal-to-noise ratio. Stroboscopic detection was used in all cases to allow a direct comparison. (A) C_α without decoupling. (B) C_α with C′ decoupling. (C) C_α with simultaneous decoupling from C′ and C_β regions. (D) C′ without decoupling. (E) C′ with C_α decoupling.

experiments (B), (E), and (C), respectively. All shaped pulses were generated using the STDISP utility in XWINNMR 3.5. The experimental results are summarized in Table 1. Stroboscopic detection was used for the reference experiments represented in (A) and (D), to allow for direct comparison with the homonuclear decoupling experiments, shown in (B), (C), and (E). The C′ region of the spectrum recorded with standard detection is represented in (F) to allow for a direct comparison with stroboscopic detection (D). The signal intensity is normalized with respect to the noise in all experiments. Working at a magnetic field strength of 600 MHz and a MAS rotation frequency of 12.5 kHz, we observe that scalar splittings are resolved for, e.g., resolved C′ and methyl resonances. Therefore, second order dipolar broadening as it is discussed by McDermott and co-worker [20] does not significantly contribute to the line width in our case. This might, however, be different for other B_0 fields or MAS rotation frequencies.

We observe a reduction in line width for Leu and Val C′ in the case of decoupling from C_α by 59 and 49 Hz, respectively, which is in the order of the C′–C_α scalar coupling, indicating good performance. In the case of decoupling C_α from C′, a line narrowing of 50.5 and 36 Hz is observed for Leu and Val C_α, respectively. Simultaneous decoupling of C′ and C_β while observing C_α results in a line narrowing of 74 and 58 Hz for Leu and Val, respectively. Previously, a line narrowing in the direct dimension in case of decoupling C_α from C′ using the spin-state selective scheme of 40–42 Hz [22], and in the indirect dimension in case of simultaneous decoupling of C_α from C′ and C_β of ca. 55 Hz [20] could be achieved at moderate spinning frequencies. The gain in sensitivity observed in the spectra upon homonuclear decoupling compared to the reference experiments (without homonuclear decoupling) is given in Fig. 2. Taking into account a factor of 0.65 which corresponds to the sensitivity losses due to stroboscopic detection, we still observe an improvement in sensitivity of, e.g., 116% for Leu C_α.

Despite the advantage of higher sensitivity and resolution, homodecoupling can cause significant Bloch–Siegert shift (BSS) of the resonances of interest [35]. In the case of decoupling C_α from C′ and C′ from C_α, no induced shifts were observed due to the large chemical shift difference between these nuclei. Double band selective decoupling causes an induced shift of the C_α and C_γ resonance frequency due to irradiation of C_β. The BSS value in this experiment for both Val and Leu C_α is 19 Hz. This value is on the order of 0.13 ppm and therefore much smaller than the line width and close to the digital resolution one obtains in multi-dimensional experiments. BSS can be compensated by using an additional symmetric pulse of the same shape having the opposite frequency offset from the signal of interest which can easily be implemented in the indirect dimension. The major limitation of this approach in the direct dimension is the short time available for RF irradiation during detection. Using a compensatory pulse significantly decreases the decoupling performance in the direct dimension (results not shown). Also, calculation of the BSS based on numerical simulations is possible [24] and can be performed for any elaborative adiabatic pulse.

The homonuclear decoupling sequence was applied to an amyloidogenic hexameric peptide (STVIIE) [36]. ^{13}C-1D spectra of ^{13}C–^{15}N uniformly labelled STVIIE with and without decoupling are presented in Figs. 3B and A, respectively. The spectrum without decoupling was acquired in the standard detection mode. The natural abundance spectrum of the peptide is shown in Fig. 3C. Comparison of the decoupled spectrum with the natural abundance and the non-decoupled spectra demonstrates the high efficiency of the decoupling scheme.

Single band ^{13}C′–$^{13}C_\alpha$ J decoupling was achieved by selective irradiation of the $^{13}C_\alpha$ region. Parameters of the employed pulse sequence are similar to those used in the previous experiments applied to the dipeptide. An adiabatic SEDUCE-1 pulse with a MLEV16 supercycle was applied with an on-resonance frequency of 59 ppm (see Fig. 3D) employing a RF field amplitude of 5 kHz and a duration of 11.5 ms. In case of continuous irradiation, the pulse has an excitation band width of 4 kHz, while windows for detection make it more selective. RF power and duration of the pulse were experimentally adjusted for optimal performance.

This approach was utilized to improve the resolution of the 2D experiment. $C^{aliphatic}$–C′ spectral regions of the PDSD ^{13}C–^{13}C correlation experiment performed with and without homonuclear decoupling are presented in Figs. 4B and A, respectively. The former spectrum

Table 1
Full line width at half height (Δ) in Hz for Nac-Val-Leu for decoupling of different spectral regions

	Δ Leu C′	Δ Val C′	Δ Val Cα	Δ Leu C_α	RF power (Hz)	Refocusing pulse duration (ms)	Supercycle	BSS (Hz)
A			111.5	125				
B			75.5	74.5	4400	12.7	Mlev16	0
C			53.5	51	8300	10.640	P9	19
D	107	101.5						
E	48	52.5			4400	12.7	Mlev16	0

Abbreviations in the table for different spectra correspond to ones used in capture of Fig. 2 (A) C_α without decoupling. (B) C_α with C′ decoupling. (C) C_α with simultaneous decoupling from C′ and C_β regions. (D) C′ without decoupling. (E) C′ with C_α decoupling.

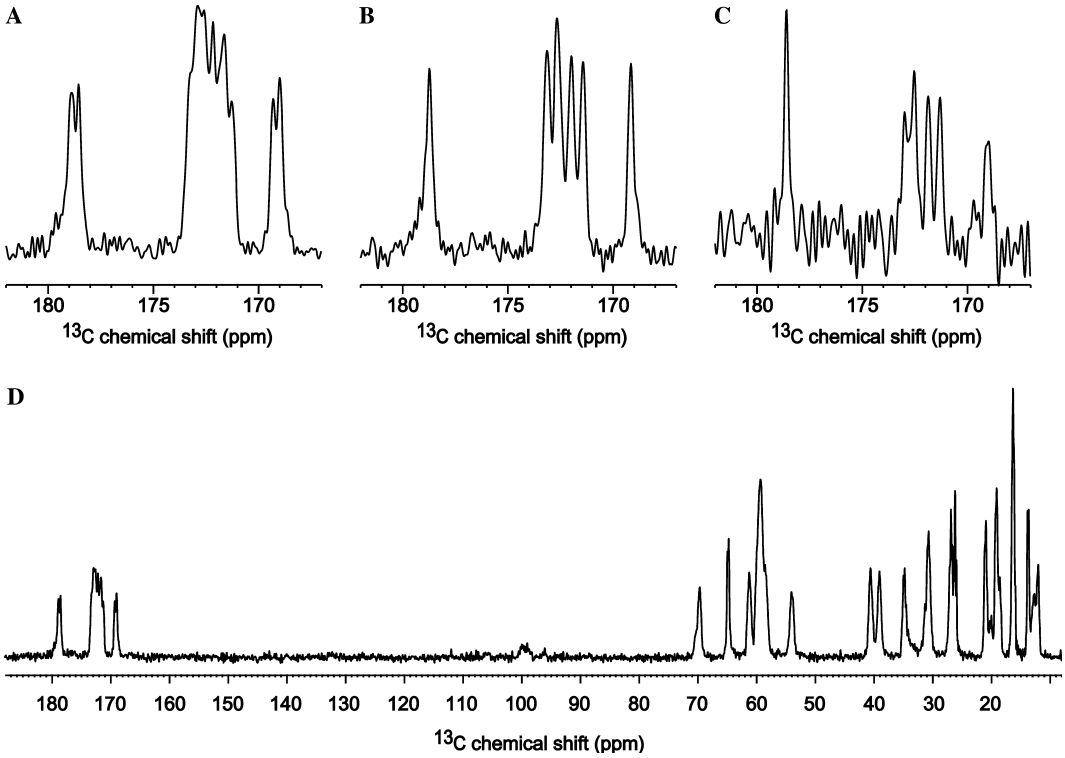

Fig. 3. ^{13}C-1D spectra of fibrillized STVIIE demonstrating the performance of ^{13}C–^{13}C homonuclear scalar decoupling. Spectra were acquired at a MAS frequency of 11 kHz, temperature of 273 K and application of a 90 kHz RF field strength for TPPM decoupling. (A) C′ region of ^{13}C–^{15}N uniformly labelled sample without homonuclear scalar decoupling (standard detection), ns = 256. (B) C′ region of ^{13}C–^{15}N uniformly labelled sample with homonuclear scalar decoupling applied to the C_α region, ns = 256. (C) Natural abundance spectrum, ns = 22,000. (D) Full spectrum of ^{13}C–^{15}N uniformly labelled sample, ns = 256. Spectra (A), (B), and (D) were recorded at the same conditions. The acquisition time in the experiments was 35 ms. The experimental time for each experiment was 8 min. The spectrum (C) was recorded using an acquisition time of 30 ms, and was recorded within 22 h. No apodization was applied for all spectra.

was recorded using the pulse sequence shown in Fig. 2B. Homonuclear J decoupling in the direct dimension was analogous to the 1D experiments. For the indirect dimension, the same pulse shape was employed, while the amplitude of the applied RF field was set to 1600 Hz due to continuity of the irradiation. The resolution achieved in the decoupling experiment allows unambiguous assignment of all resonances, especially C_α–C′ correlations, which was not possible before. The standard PDSD experiment demonstrates for most peaks resolved J couplings, making the spectrum more confusing for interpretation, especially for the regions with spectral overlap. In the decoupled spectrum, we count only six C_α–C′ correlations, while seven would be expected. The missing C′ resonance is broadened due to chemical exchange between different conformations (data not shown). Analysis of the chemical shifts of the cross-peaks indicates that the missing resonance belongs to the side chain glutamic acid carboxyl.

The experiments obviously show that decoupling during acquisition is useful for improving the spectral resolution in the direct dimension. J decoupling is highly efficient when J is comparable or larger than the natural line width. In cases where the J scalar coupling is resolved, decoupling results in a reduction of the number of peaks by a factor of 2^n, where n corresponds to the number of decoupled spins. This can dramatically enhance the resolution in complicated spectra. If the sum of scalar couplings $\sum J_i$ exceeds the natural line width, ideal decoupling decreases the line width by $\sum J_i$. In this case, the presented experimental approach gives the theoretical value for a signal-to-noise ratio enhancement in case of full decoupling as

$$\frac{S}{N} = k\frac{S}{N}\bigg|_0 2^n, \tag{2}$$

where $S/N|_0$ denotes the signal-to-noise ratio of the spectrum without decoupling. The factor k describes the signal-to-noise ratio decrease due to stroboscopic detection and n corresponds to the number of decoupled spins. While spin-state-selective schemes yield a signal-to-noise ratio

$$\frac{S}{N} = h\frac{S}{N}\bigg|_0 \sqrt{2^n}, \tag{3}$$

where $S/N|_0$ denotes the signal-to-noise ratio of the spectrum without decoupling. The factor h reflects the signal decrease during the preparation period, which

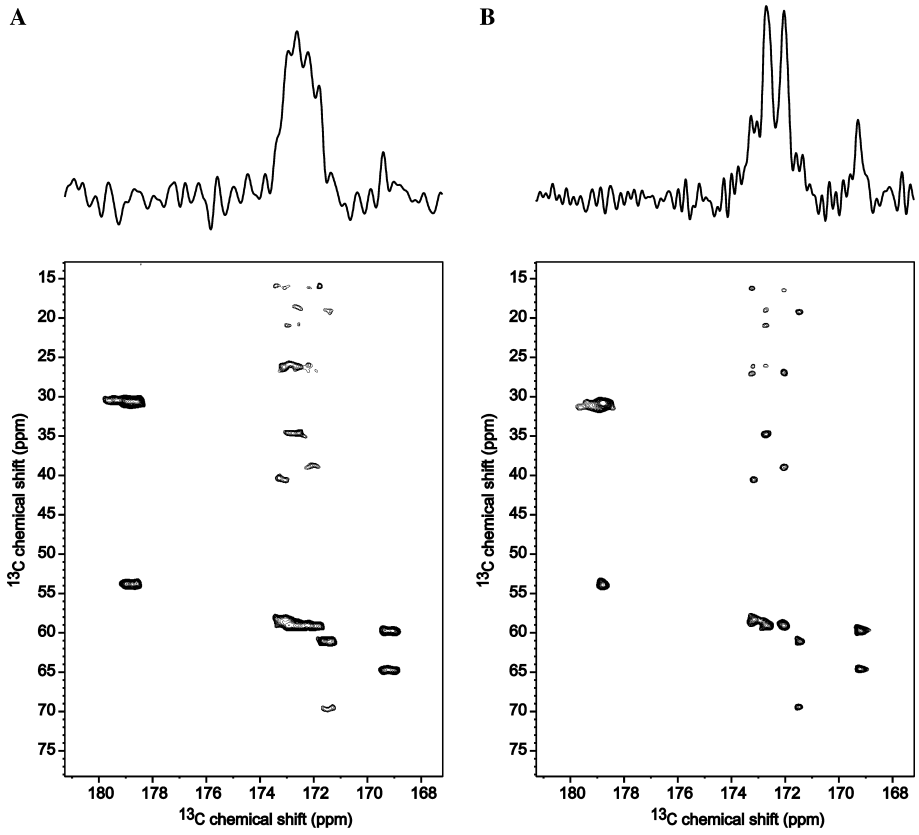

Fig. 4. $C^{aliphatic}$–C′ regions of two PDSD spectra of fibrillized u-[^{13}C–^{15}N] STVIIE using a mixing time of 15 ms. (A) Reference experiment, without homonuclear J decoupling. (B) Experiment recorded with homonuclear J decoupling in both dimensions according to the pulse sequence represented in Fig. 2B. The row on top of the spectra represents a trace through the C_α spectral region at 59.1 ppm. All spectra were recorded at the same experimental conditions. The MAS frequency was set to 11 kHz, temperature was adjusted to 273 K and TPPM of 90 kHz was used for heteronuclear decoupling in both dimensions. An acquisition time of $t_1^{max} = 10$ ms and $t_2^{max} = 30$ ms was used for the indirect and direct dimension, respectively, with TPPI [37] for phase sensitive detection. Both spectra were processed by applying a sine-bell function phase shifted by $\pi/3$ and by $\pi/3.5$ in t_1 and in t_2, respectively. Total experimental time for both spectra was 12 h. Plot levels in both spectra are chosen to be slightly above noise level.

for moderate MAS frequencies of 10–15 kHz is on the order of 0.4–0.85, depending on the nucleus [22], n refers to the number of decoupled spins 1/2.

In conclusion, we have shown that application of homonuclear decoupling is feasible during detection. This decoupling scheme increases the resolution of the carbon resonances up to a factor of 2–2.5. At the same time, sensitivity can be moderately increased (up to a factor 1.2). We assume that this strategy turns out to be useful for larger biomolecules like, e.g., membrane proteins, where spectral overlap is critical.

References

[1] F. Castellani, B.J.v. Rossum, A. Diehl, K. Rehbein, H. Oschkinat, Structure of a protein determined by solid-state magic-angle spinning NMR spectroscopy, Nature 420 (2002) 98–102.
[2] C.M. Rienstra, L. Tucker-Kellogg, C.P. Jaroniec, M. Hohwy, B. Reif, T. Lozano-Peres, B. Tidor, R.G. Griffin, De novo structure determination of peptides and proteins with high resolution solid state MAS NMR, Proc. Natl. Acad. Sci. USA 99 (2002) 10260–10265.
[3] J. Pauli, B.J.v. Rossum, H. Forster, H.J.M.d. Groot, H. Oschkinat, Sample optimization and identification of signal patterns of amino acid side chains in 2D RFDR spectra of the alpha-spectrin SH3 domain, J. Magn. Reson. 143 (2000) 411–416.
[4] M. Ernst, M.A. Meier, T. Tuherm, A. Samoson, B.H. Meier, Low-power high-resolution solid-state NMR of peptides and proteins, J. Am. Chem. Soc. 126 (2004) 4764–4765.
[5] M. Ernst, A. Samoson, B.H. Meier, Low-power XiX decoupling in MAS NMR experiments, J. Magn. Reson. 163 (2003) 332–339.
[6] A. Bielecki, A.C. Kolbert, M.H. Levitt, Frequency-switched pulse sequence—homonuclear decoupling and dilute spin NMR in solids, Chem. Phys. Lett. 155 (1989) 341–346.
[7] E. Vinogradov, P.K. Madhu, S. Vega, High-resolution proton solid-state NMR spectroscopy by phase-modulated Lee–Goldburg experiment, Chem. Phys. Lett. 314 (1999) 443–450.
[8] A.E. Bennett, C.M. Rienstra, M. Auger, K.V. Lakshmi, R.G. Griffin, Heteronuclear decoupling in rotating solids, J. Chem. Phys. Lett. 103 (1995) 6951–6958.
[9] M. Rosay, J.C. Lansing, K.C. Haddad, W.W. Bachovchin, J. Herzfeld, R.J. Temkin, R.G. Griffin, High-frequency dynamic nuclear polarization in MAS spectra of membrane and soluble proteins, J. Am. Chem. Soc. 125 (2003) 13626–13627.
[10] B. Reif, R.G. Griffin, H-1 detected H-1, N-15 correlation spectroscopy in rotating solids, J. Magn. Reson. 160 (2003) 78–83.
[11] E.K. Paulson, C.R. Morcombe, V. Gaponenko, B. Dancheck, R.A. Byrd, K.W. Zilm, Sensitive high resolution inverse detection

NMR spectroscopy of proteins in the solid state, J. Am. Chem. Soc. 125 (2003) 15831–15836.
[12] V. Chevelkov, B.J.v. Rossum, F. Castellani, K. Rehbein, A. Diehl, M. Hohwy, S. Steuernagel, F. Engelke, H. Oschkinat, B. Reif, H-1 detection in MAS solid-state NMR spectroscopy of biomacromolecules employing pulsed field gradients for residual solvent suppression, J. Am. Chem. Soc. 125 (2003) 7788–7789.
[13] A. McDermott, T. Polenova, A. Bockmann, K.W. Zilm, E.K. Paulsen, R.W. Martin, G.T. Montelione, Partial NMR assignments for uniformly (C-13, N-15)-enriched BPTI in the solid state, J. Biomol. NMR 16 (2000) 209–219.
[14] J. Cavanagh, W. Fairbrother, A.G. Palmer, N.J. Skelton, Protein NMR Spectroscopy: Principles and Practice, Academic Press, New York, 1996, pp. 480–481.
[15] M. Sattler, J. Schleucher, C. Griesinger, Heteronuclear multidimensional NMR experiments for the structure determination of proteins in solution employing pulsed field gradients, Prog. NMR Spectrosc. 34 (1999) 93–158.
[16] D.M. LeMaster, D.M. Kushlan, Dynamical mapping of *E. coli* thioredoxin via C-13 NMR relaxation analysis, J. Am. Chem. Soc. 139 (1996) 9255–9264.
[17] M. Hong, K. Jakes, Selective and extensive C-13 labeling of a membrane protein for solid-state NMR investigations, J. Biomol. NMR 14 (1999) 71–74.
[18] R. Brüschweiler, C. Griesenger, O.W. Sorensen, R.R. Ernst, Combined use of hard and soft pulses for omega-1 decoupling in two-dimensional NMR-spectroscopy, J. Magn. Reson. 78 (1988) 178–185.
[19] S.K. Straus, T. Bremi, R.R. Ernst, Resolution enhancement by homonuclear *J* decoupling in solid-state MAS NMR, Chem. Phys. Lett. 262 (1996) 709–715.
[20] T.I. Igumenova, A.E. McDermott, Improvement of resolution in solid state NMR spectra with *J*-decoupling: an analysis of lineshape contribution in uniformly 13-C enriched amino acids and proteins, J. Magn. Reson. 164 (2003) 270–285.
[21] L. Duma, S. Hediger, B. Brutscher, A. Boekmann, L. Emsley, Resolution enhancement in multidimensional solid-state NMR spectroscopy of proteins using spin-state selection, J. Am. Chem. Soc. 125 (2003) 11816–11817.
[22] L. Duma, S. Hediger, A. Lesage, L. Emsley, Spin-state selection in solid-state NMR, J. Magn. Reson. 164 (2003) 187–195.
[23] M.D. Sørensen, A. Meissner, O.W. Sørensen, C-13 natural abundance (SE)-E-3 and (SCT)-C-3 experiments for measurement of *J* coupling constants between C-13(alpha) or H-1(alpha) and other protons in a protein, J. Magn. Reson. 137 (1999) 237–242.
[24] H. Matsuo, E. Kupce, H.J. Li, G. Wagner, Increased sensitivity in HNCA and HN(CO)CA experiments by selective C-beta decoupling, J. Magn. Reson. B 113 (1996) 91–96.
[25] H. Matsuo, E. Kupce, G. Wagner, Resolution and sensitivity gain in HCCH-TOCSY experiments by homonuclear C-beta decoupling, J. Magn. Reson. B 113 (1996) 190–194.
[26] W. Bermel, I. Bertini, I.C. Felli, R. Kummerle, R. Pierattelli, C-13 direct detection experiments on the paramagnetic oxidized monomeric copper, zinc superoxide dismutase, J. Am. Chem. Soc. 125 (2003) 16423–16429.
[27] N.C. Nielsen, H. Bildsoe, H.J. Jakobsen, M.H. Levitt, Double-quantum homonuclear rotary resonance: efficient dipolar recovery in magic-angle spinning nuclear magnetic resonance, J. Chem. Phys. 101 (1994) 1805–1812.
[28] T.G. Oas, R.G. Griffin, M.H. Levitt, Rotary resonance recoupling of dipolar interactions in solid-state nuclear magnetic resonance spectroscopy, J. Chem. Phys. 89 (1988) 692–695.
[29] M.A. McCoy, L. Mueller, Selective shaped pulse decoupling in NMR–homonuclear [C-13] carbonyl decoupling, J. Am. Chem. Soc. 114 (1992) 2108–2112.
[30] M.A. McCoy, L. Mueller, Selective decoupling, J. Magn. Reson. A 101 (1993) 122–130.
[31] G.A. Morris, R. Freeman, Selective excitation in Fourier-transform nuclear magnetic resonance, J. Magn. Reson. 29 (1978) 433–462.
[32] M.H. Levitt, R. Freeman, Composite pulse decoupling, J. Magn. Reson. 43 (1981) 502–507.
[33] H. Cho, J. Baum, A. Pines, Iterative maps with multiple fixed-points for excitation of 2 level systems, J. Chem. Phys. 86 (1987) 3089–3106.
[34] H.M. Cho, R. Tycko, A. Pines, J. Guckenheimer, Iterative maps for bistable excitation of 2-level systems, Phys. Rev. Lett. 56 (1986) 1905–1908.
[35] F. Bloch, A. Siegert, Magnetic resonance for nonrotating fields, Phys. Rev. 57 (1940) 522–527.
[36] M.L.d.l. Paz, K. Goldie, J. Zurdo, E. Lacroix, C.M. Dobson, A. Hoenger, L. Serrano, Proc. Natl. Acad. Sci. USA 99 (2002) 16052–16057.
[37] R.R. Ernst, G. Bodenhausen, A. Wokaun, Principles of Nuclear Magnetic Resonance in One and Two Dimensions, Clarendon, Oxford, 1987.